Journal of Applied Polymer Science

Dispersion Control of Immiscible Polymer Blend Using Selective Heating by Infrared Laser Irradiation

Takushi Saito, Tatsuya Kawaguchi, Isao Satoh
Department of Mechanical and Control Engineering, Tokyo Institute of Technology, Tokyo, Japan
Correspondence to: T. Saito (E-mail: tsaito@mep.titech.ac.jp)

ABSTRACT: In this study, a selective heating technique by irradiating an infrared laser to an immiscible polymer blend was proposed to actively control the distribution of the dispersed phase in the blend. In the technique, the viscosity ratio between the matrix and dispersed phases was not changed by the molecular weight or shear rate but was changed by the controlled temperature distribution due to selective heating. The feasibility of the proposed technique was investigated through a numerical simulation of the temperature field and an experimental study using a test blend. The results showed that the technique successfully caused the deformation of relatively large droplets and enhanced the micro-scale dispersion. It was also confirmed that the droplet size of the dispersed phase could be estimated by a simple method similar to the conventional technique: the chart of capillary number change with respect to the viscosity ratio. From the obtained results, it was concluded that the technique proposed in this study is a promising candidate for the development of a new blend process. © 2013 Wiley Periodicals, Inc. J. Appl. Polym. Sci. 129: 3606–3612, 2013

KEYWORDS: blends; thermoplastics; irradiation

Received 24 October 2012; accepted 24 January 2013; published online 1 March 2013
DOI: 10.1002/app.39110

INTRODUCTION

Polymer blend techniques for mixing different polymeric materials are important, because they help to improve the physical properties of the blended materials at a low cost.[1] For example, it is well known that the dispersion of a small amount of elastomer improves the toughness of brittle materials.[2,3] In a polymer blend system, it is preferable for dispersion to be minute and uniform in order to obtain homogeneous physical properties.[4,5] However, the local distribution of the dispersed phase and its deformation depends on the products' shape and the process history. Jarus et al. reported that the weld-line strength of a molded product made by a blend material was influenced by the deformation ratio of the dispersed phase.[6] Therefore, a technique that can independently control the distribution of the dispersed phase from outside the system is an important solution to this problem.

In an immiscible polymer blend in the molten state, the viscosity difference and the interfacial tension between the matrix and dispersed phases affect the dispersion as similar to the addition of nanoparticles.[7,8] The viscosity ratio of the matrix and dispersed phases can be adjusted by changing the molecular weight of the materials and by adding a compatibilizer that would lower the interfacial tension. However, the preparation of many materials with different viscosities complicates the blending process. Preparing all the combinations of compatibilizer for blend materials is not cost-effective. Moreover, the compatibilizer does not affect the mixing process at the early stages, because it only begins to work when the minor phase reaches the micro-scale.

It is generally known that the viscosity of molten polymer is a function of the temperature and shear rate.[9] Therefore, the melt viscosity ratio of the materials depends on the mixing conditions, which in turn affects the dispersion process. In order to realize a positive impact on the viscosity ratio via shear rate control, the gap between the screw and cylinder wall needs to be decreased with high precision. The viscosity ratio cannot be controlled via heating, because the conductive heating of the electric heater causes a temperature rise in both the dispersed phase and the matrix phase. These facts suggest that a technique that alters the physical properties is needed to control the size of the dispersed phase by changing the melt viscosity ratio. For example, selectively heating the high-viscosity dispersed phase would result in the matrix and dispersed phases having a matched viscosity. This is an innovative technique for the control of the dispersed phase, and it mitigates the issues of the conventional techniques described above. As a one candidate, ultrasonic vibration might be used for this kind of purpose.[10,11] However, the use of ultrasonic vibration usually requires the strict design of the facilities.

Table I. Material Properties

	PE with carbon black (dispersed phase)	PS (matrix phase)
Density (kg m^{-3})	922	1050
Specific heat (J kg^{-1} K^{-1})	2300	1300
Thermal conductivity (W m^{-1} K^{-1})	0.36	0.19
Absorption coefficient (m^{-1}) @ 1063 nm	102,000	46.4
Melt viscosity (Pa s) @ 180°C, 1.0 rad s^{-1}	8200	6800

In this study, a technique that selectively heats a target area is proposed by exploiting the different radiation absorption coefficients of each material. The viscosity ratio between the matrix and dispersed phases changes according to the temperature distribution. This method can actively control the dispersion progress, because the intensity of the radiation energy supplied from the outside of the system is independent of the mixing process itself. First, a numerical simulation that estimates the temperature distribution in the blend was carried out to obtain the characteristic temperature distribution of the technique. In the experimental study, a model blend was extruded from a test die, and the deformation behavior of the dispersed phase was observed using an optical microscope. The effect of the technique on the dispersed phase was quantitatively evaluated by scanning electron microscopy (SEM), and the characteristics of the technique are discussed herein, from the viewpoint of dispersion control.

SELECTIVE HEATING BY LASER IRRADIATION

The one-dimensional attenuation of monochromatic radiation that is transmitted in a semi-transparent medium is described by the Lambert–Beer law as follows:

$$I = I_0 \exp(-\beta x) \tag{1}$$

where I, I_0, β, and x are the radiation intensity at local position, initial radiation intensity, radiation absorption coefficient, and penetration length, respectively. If the scattering of radiation in the medium is neglected, the attenuated radiation energy is equal to the thermal energy generated in the medium; this is the simplest approximation of radiation heating. However, the difference between the monomer structure and the additive agents greatly influences the radiation absorption coefficient. Therefore, the selective heating of the dispersed phase in a blend can be realized by carefully selecting the type of laser corresponding to materials with different radiation absorption coefficients.

For the experimental apparatus design, one part of the wall enclosing the test section needs to be optically transparent to allow the radiation energy to be introduced to the system. Although some crystalline materials for optical application have a high transmittance in the infrared wavelength region, a heat-resistant glass was used in this study because it had sufficient transparency, and the wavelength of the infrared radiation was 1.06 μm (Nd:YAG laser).

ESTIMATION OF THE TEMPERATURE DISTRIBUTION

Test Blend Used in This Study

The physical properties of the materials used in this study are summarized in Table I. In the test blend, polyethylene (PE) and polystyrene (PS) were the dispersed phase and the matrix phase, respectively. Carbon black powder was added to the PE at 2 wt % prior to mixing, to increase the radiation absorption coefficient of the dispersed phase. The blend was 97 wt % PS and 3 wt % PE. A thin film of each material was produced to quantitatively determine the radiation absorption coefficient by using a spectrometer (UV1600PC, Shimadzu Corp., Kyoto, Japan).

Scheme of the Numerical Simulation

To obtain the fundamental information of the experimental conditions, a simulation of unsteady heat transfer in a blend material was performed in a two-dimensional coordinate system by using the finite difference method. Figure 1 shows the computational domain used, and the temperature distribution was estimated from half of the domain by considering the symmetry along the transmission direction of the radiation (the x-axis). The size of the computational domain, defined as L, was varied from 3000 to 400 μm, and thus, the diameter of the dispersed phase, which was estimated as $L/5$, was varied from 600 to 80 μm. This situation was considered to be equivalent from the initial to the middle stages in the actual melt mixing. The computational domain was divided by a square mesh, and the division numbers of the x- and y-axes were 100 and 50, respectively. The area ratio of the dispersed phase was 3.14%.

In the numerical simulation, the radiation heating and the thermal diffusion in the domain were calculated with the assumptions of a negligible flow and negligible deformation. Neither the scattering of the laser beam nor the internal radiation heat transfer due to the temperature distribution in the domain was considered in the calculation. The temperature dependence of the physical properties was also neglected. After applying these simplifications, the governing equations for the temperature distribution in the two-dimensional coordinate system can be written as follows:

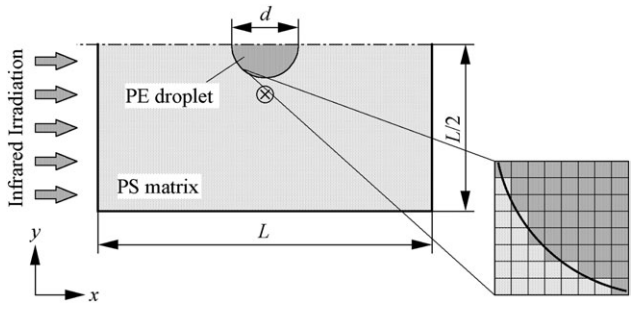

Figure 1. Calculation domain of the numerical simulation for temperature distribution.

Table II. Calculation and Experimental Conditions

Initial melt temperature (°C)	180, 190, 210, 230
Melt flow rate (cm s^{-1}) (only for the experiment)	15 (averaged value)
Radiation intensity (W cm^{-2})	0, 10, 20, 31
Time step (ms) (only for the simulation)	5
Heating duration (s)	0.065

$$\rho_{sub} c_{sub} \frac{\partial T_{sub}}{\partial t} = \frac{\partial}{\partial x}\left(k_{sub}\frac{\partial T_{sub}}{\partial x}\right) + \frac{\partial}{\partial y}\left(k_{sub}\frac{\partial T_{sub}}{\partial y}\right) + S_{sub} \quad (sub: m \text{ or } d) \tag{2}$$

$$S_{sub} = \left|\frac{\partial I}{\partial x}\right| = \beta_{sub} I_0 \exp(-\beta_{sub} x) \tag{3}$$

where ρ, c, k, β, T, t, and S denote the density, specific heat, thermal conductivity, radiation absorption coefficient, temperature, time, and heat generation by radiation heating, respectively. The subscripts m and d indicate the matrix phase and the dispersed phase, respectively. The interface conditions of the calculation domain are summarized as follows.
(Outer edge of the calculation domain)

$$\frac{\partial T}{\partial x} = 0 \quad \left(\text{at } x = 0, \quad 0 \le y \le \frac{L}{2} \quad \text{and at } x = L, \quad 0 \le y \le \frac{L}{2}\right) \tag{4}$$

$$\frac{\partial T}{\partial y} = 0 \quad \left(\text{at } 0 \le x \le L, \quad y = 0 \quad \text{and at } 0 \le x \le L, \quad y = \frac{L}{2}\right) \tag{5}$$

(Interfacial condition between the matrix and dispersed phases)

$$k_m \frac{\partial T_m}{\partial x} = k_d \frac{\partial T_d}{\partial x}, \quad k_m \frac{\partial T_m}{\partial y} = k_d \frac{\partial T_d}{\partial y}, \quad T_m = T_d \tag{6}$$

The calculation conditions are summarized in Table II. In the calculation, the temperature of the domain was set at the initial melt temperature. Then, the change of the temperature distribution after time 0 was estimated and discussed.

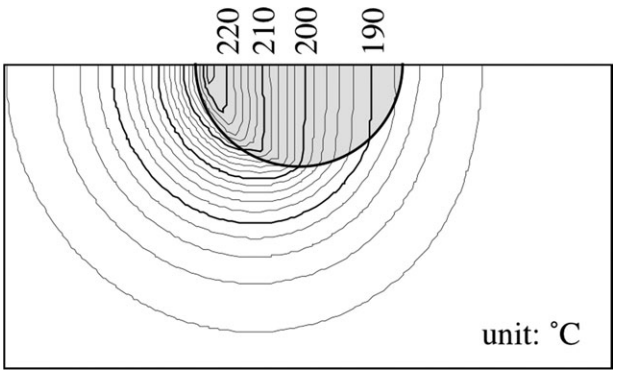

Figure 2. An example of the estimated temperature distribution (L = 1 mm, d = 0.2 mm, I_0 = 31 W cm^{-2}, initial melt temperature = 180°C).

Results Obtained from the Calculation

Figure 2 shows an example temperature distribution obtained by the simulation. The diameter of the droplet shown in this figure was 200 μm, and the initial temperature, T_0, was 180°C. The radiation energy was introduced from the left side of the domain for 60 ms. The temperature rise of the droplet surface facing the irradiation was measurable in this short time. This leads to the expectation that the distribution of the dispersed phase in the experimental study would begin in warmer region, where the viscosity was lowered.

The variation of the representative temperatures of the matrix and dispersed phases are shown in Figure 3 as a function of the diameter of the dispersed phase. The temperature of the dispersed phase was the maximum value in the calculation domain, and the temperature of the matrix phase was the value of the point marked in Figure 1. As shown in this figure, the effectiveness of selective heating lessened with the decrease of the droplet diameter. There are two reasons for the decrease in effectiveness. First, the relative thermal diffusion increased due to the miniaturization of the domain. Second, the amount of radiation energy absorbed in the dispersed phase decreased with the decreasing droplet size. As a result, the proposed technique that lessens the viscosity difference between the matrix and dispersed phases is most effective in the early stage of the dispersion process (when the size of dispersed phase >100 μm).

DISPERSION CONTROL USING SELECTIVE RADIATION HEATING

Experimental Apparatus and Procedure

A test blend consisting of the matrix phase PS and the dispersed phase PE with carbon powder was used to investigate the effectiveness of the proposed technique. The shear viscosity of each material is shown in Figure 4. The viscosity of PE was higher than that of PS for a wide range of temperatures and shear rates, except for high shear rates.

The polymer blend was extruded from a simple channel, and the radiation energy was irradiated onto the blend (Figure 5).

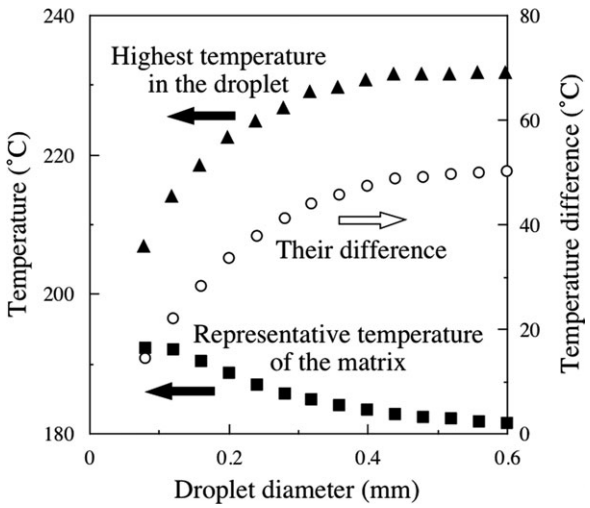

Figure 3. Temperature change of the representative points of the matrix and the dispersed phases.

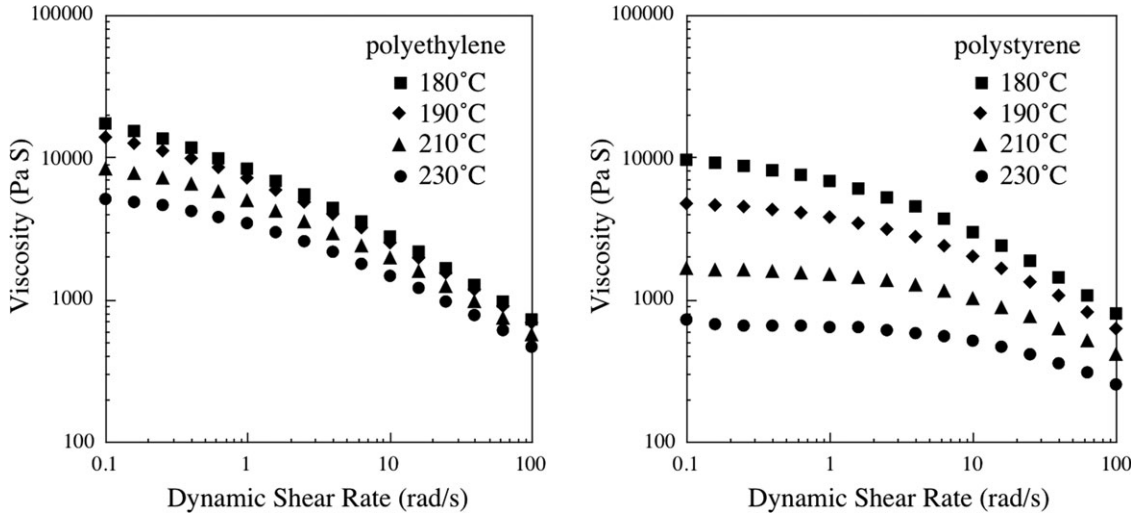

Figure 4. Measured shear viscosity of the used materials.

The cross section of the flow channel was 4 mm wide and 2 mm deep, and the radiation energy was introduced from the center of the side of the channel. A window made of heat-resistant glass was installed to directly irradiate the polymer blend, which also enabled observation of the blend flow by using an optical microscope (VH5900, KEYENCE Co., Osaka, Japan). An Nd:YAG laser (825M, Lee Laser, FL, USA) was the radiation energy source, and its oscillation wavelength was 1.06 μm, and the maximum power was 31 W. Pellets of PS and PE were mixed in the dry condition, and then they were poured into the hopper of the plasticizing unit. Therefore, the dispersion of the PE phase progressed with the assistance of the plasticizing screw, and the test section with the selective radiation heating would enhance the dispersion further. The average shear rate in the test section was calculated from the running speed of the plasticizing unit, which was 115 s^{-1}, based on the equivalent hydraulic radius. The experimental conditions were determined according to the conditions listed in Table II.

The extruded blend was immediately cooled in a water bath to freeze the internal structure. A thin specimen was cut along the flow direction, and the PS was dissolved using xylene for obtaining PE droplets. The shape of the PE droplets was observed by SEM (JSM6301F, JEOL, Tokyo, Japan).

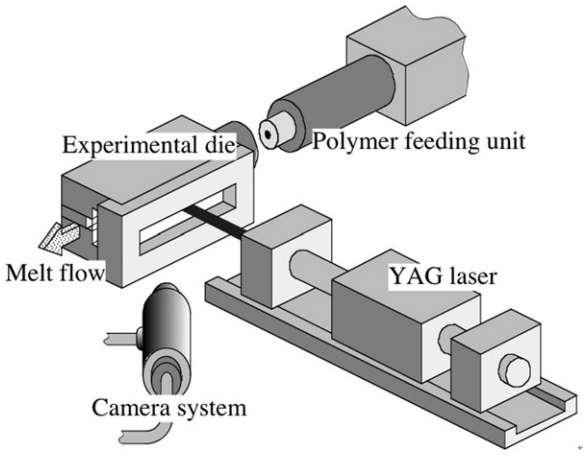

Figure 5. Experimental apparatus used in this study.

Observation of Droplet Deformation

In the mixing process of the blend material, the dispersed phase first stretches along the flow direction due to the shear flow, and it then disperses into tiny droplets due to the interfacial instability.[12] The effect of the radiation heating on the droplet deformation was evaluated macroscopically by observing the blend flow in the test section. In the experiment, the deformation of the droplets with a diameter of approximately 0.5 mm was selectively observed. Figure 6 shows the deformation degree of the droplets along the flow length position. The vertical axis denotes the ratio between the longitudinal and lateral lengths of a droplet, and thus, the increase of the ratio indicates a higher

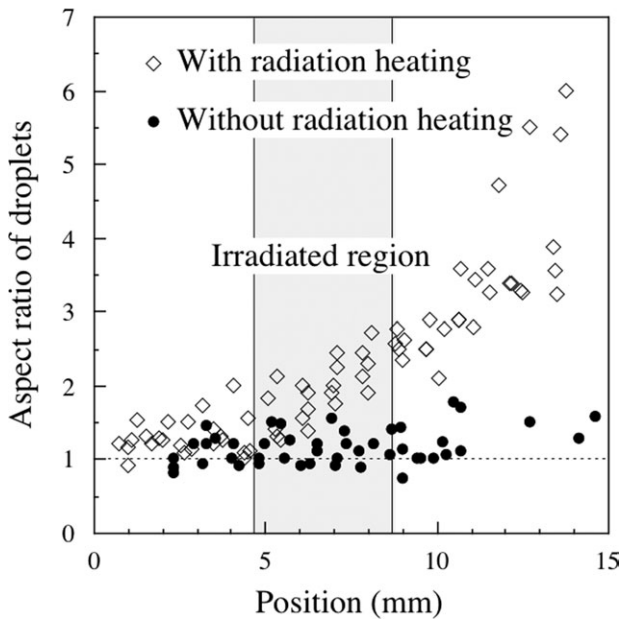

Figure 6. Aspect ratio variation of the observed droplets.

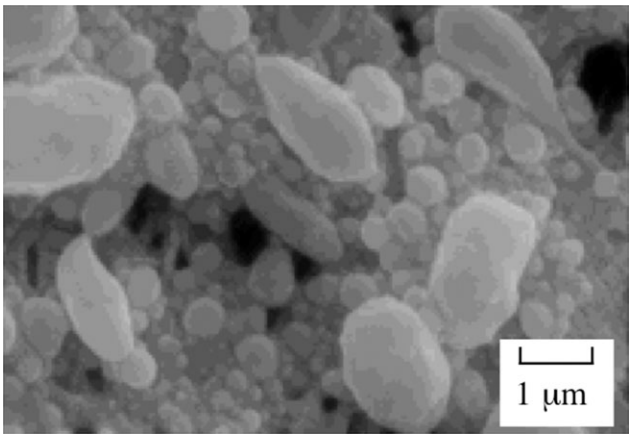

Figure 7. SEM image of the dispersed droplets.

development of the deformation. The results contain a certain deviation caused by the droplet size variation and the uncertainty of the droplet depth position in the flow path. However, the selective radiation heating considerably accelerated the droplet deformation. From the results, the effectiveness of the proposed technique was confirmed for droplets in the size range of a few hundred microns.

Distribution of the Droplet Size of the Dispersed Phase

To discuss the micro-scale structure of the blend material, it is important to know the dispersion of the relatively large droplets observed in the previous section. Therefore, the shape and size of the dispersed phase in the extruded sample were quantitatively measured by SEM. Although the actual shape of the dispersed droplets was somewhat complex (Figure 7), they were presumed to be ellipsoid in the image processing. The projected area and peripheral length of the dispersed droplets were measured by the image processing software, and the number of droplets examined in each measurement was greater than 100.

The relationship between the projected area and peripheral length without the laser irradiation is shown in Figure 8(a). The results of different initial temperatures are indicated in this figure, and a solid line corresponds to the data of an ideal sphere. A departure of the data point from the solid line indicated an increase in droplet deformation. The shape of the droplets became more spherical with the decrease in diameter because of the interfacial tension. A precise investigation showed that the droplet deformation was suppressed by increasing the initial temperature of the polymer melt. This result is reasonably understood by considering the dependency of the melt viscosity on the temperature (Figure 4). In the temperature range from 190 to 210°C, the viscosity of PE had a lower temperature dependency than that PS. As a result, the viscosity difference between PS and PE was large at 210°C, causing PE to behave as a relatively firm domain in this condition.

The relationship between the projected area and peripheral length with the application of selective radiation heating is shown in Figure 8(b). Nearly, all the data points were on the solid line for a wide range of droplet diameters, regardless of the initial melt temperature. This result seems to indicate that the proposed technique did not enhance the deformation of the dispersed phase. To understand the meaning of this result, the distribution of the droplet diameter with and without the radiation heating was quantitatively investigated (Figure 9). The number of the droplets with a diameter of 1.0 μm or greater was approximately half after the selective radiation heating, though the number of droplets with a diameter smaller than 0.3 μm was increased. From this result, the data shown in Figure 8 can be better explained with the reasoning that the dispersed phase deformed by selective radiation heating was rapidly broken into smaller droplets.

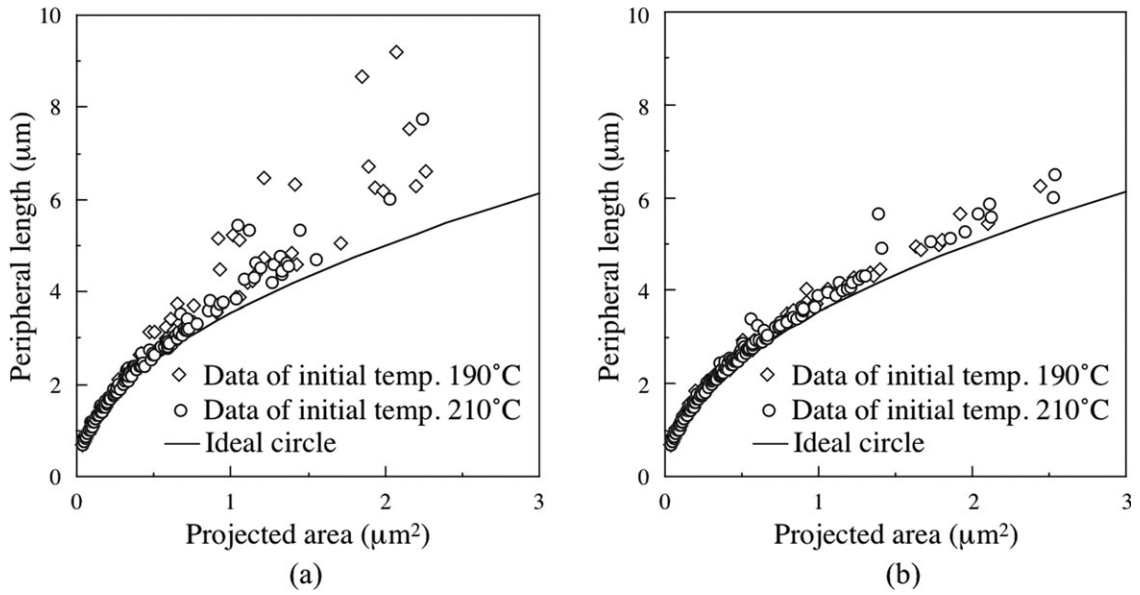

Figure 8. Peripheral length variation with respect to the projected area of the droplets: (a) without radiation heating and (b) with radiation heating at an intensity of $I_0 = 20$ W cm^{-2}.

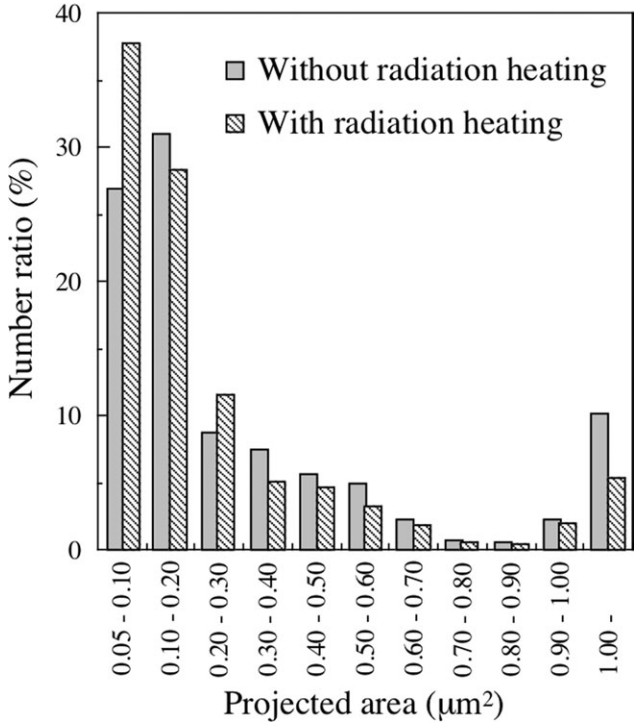

Figure 9. Effect of laser irradiation on the diameter distribution of the dispersed droplets (initial melt temperature = 180°C, I_0 = 0, 20 W cm^{-2}).

Control of the Droplet Dispersion

The experimental results showed that dispersion improvement was achieved by the proposed technique. Therefore, the diameter control of the dispersed droplets is discussed here by utilizing the results of numerical simulation, which was described in "Estimation of the temperature distribution" section. The mean diameter of the dispersed n droplets, d_{mean}, is regarded as the index of the dispersion progress and is calculated from the following equation using the droplet area, A_n, obtained by SEM.

$$d_{\text{mean}} = \frac{1}{n}\sum_{i=1}^{n}\sqrt{\frac{4A_n}{\pi}} \tag{7}$$

The capillary number, Ca, is often used to determine whether a droplet will disperse. Thus, this number provides the minimum diameter estimate of the dispersed phase droplets:

$$\text{Ca} = \frac{\tau d_{\text{mean}}}{G} \tag{8}$$

where τ and G are the shear stress and interfacial tension, respectively. Because the dispersion of the droplets is influenced by the viscosity ratio between the matrix and dispersed phases, Ca is a function of the viscosity ratio. By assuming that the shear stress is obtained by multiplying the average shear rate by the viscosity of the matrix phase, Ca can be rewritten as follows:

$$\text{Ca} = f\left(\frac{\eta_d}{\eta_m}\right) = \frac{\eta_m \dot{\gamma} d_{\text{mean}}}{G} \tag{9}$$

Therefore, the value of Ca changes with the viscosity ratio, even if the shear stress and the interfacial tension are constant. Grace introduced this idea as the critical capillary number.[13] According to this equation, it was expected that the experimental results obtained in this study would be arranged in a simple relation.

Because selective radiation heating actively controls the dispersion by varying the viscosity ratio of the matrix and dispersed phases, the relation between the viscosity ratio and Ca was investigated to evaluate the results synthetically. Ca is regarded as the dimensionless diameter of the dispersed droplets. The representative viscosities of the matrix and dispersed phases were calculated by the temperature obtained as described in "Estimation of the temperature distribution" section: the shear rate was calculated from the experimental conditions. As an example, the change in Ca with the viscosity ratio, which is actively altered the selective radiation heating at the initial temperature of 210°C, is shown in Figure 10. The mean diameter of the dispersed droplets decreased as a result of increasing the radiation intensity, because the viscosity dropped due to the higher intensity. However, the excessive radiation intensity (30.6 W cm^{-2}) hindered the PE from dispersion. From the results, a radiation intensity of approximately 20 W cm^{-2} was gathered to be the optimum condition for dispersion enhancement in the range of conditions examined.

Next, the results that include not only the radiation intensity but also the temperature change of the matrix phase were examined. Figure 11 demonstrates the relationship between the viscosity ratio and Ca that was obtained at a variety of conditions, such as different radiation intensities and the melt temperatures of the matrix phase. The solid line in the graph is Ca, which gives the minimum droplet size at a corresponding condition. According to the concept reported by Wu,[14] the relation within the examined range is described as follows:

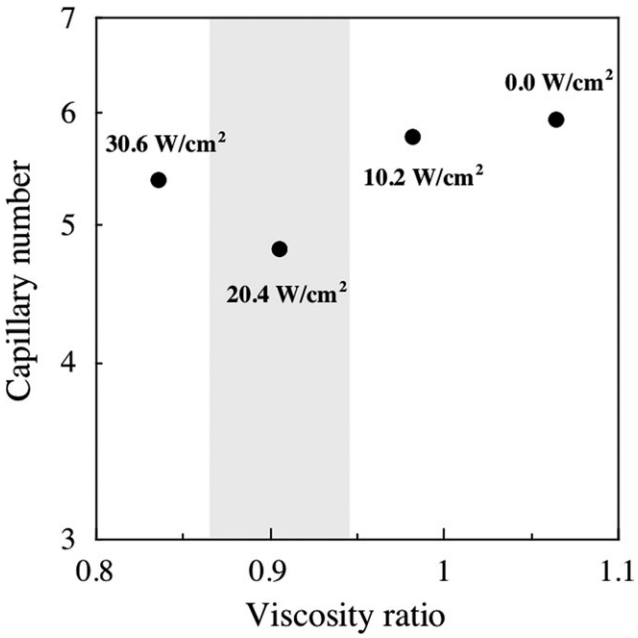

Figure 10. Ca variation with respect to the viscosity ratio.

Applied Polymer SCIENCE

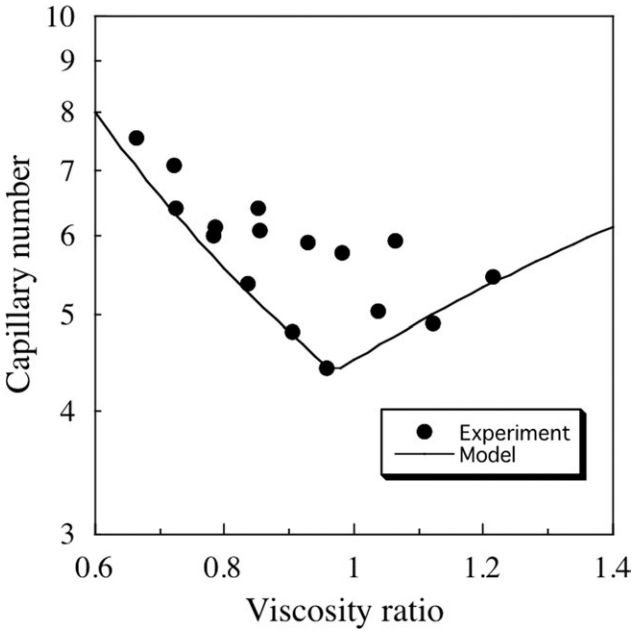

Figure 11. Scatter diagram of Ca under various conditions.

$$\mathrm{Ca} = f\left(\frac{\eta_d}{\eta_m}\right) = 4.2\left(\frac{\eta_d}{\eta_m}\right)^{-1.26} \quad \text{where} \quad \frac{\eta_d}{\eta_m} < 0.96 \tag{10}$$

$$\mathrm{Ca} = f\left(\frac{\eta_d}{\eta_m}\right) = 4.5\left(\frac{\eta_d}{\eta_m}\right)^{0.92} \quad \text{where} \quad \frac{\eta_d}{\eta_m} > 0.96 \tag{11}$$

As shown in the equations, the optimum viscosity ratio for the system was 0.96. These results indicate that achieving the distribution of the dispersed phase by the proposed technique can be controlled by the same concepts as conventional processes, given the temperatures and shear rates of the system. Moreover, the defining feature of this technique is that blend control can be achieved separately from the mixing conditions, such as the screw speed or the melt temperature, because the irradiation conditions are set independently from the mixing device.

CONCLUSIONS

In this study, the use of the laser irradiation was proposed to actively control the dispersion process of the blend material. This method enables the selective heating of the dispersed phase, which allows the matching of the viscosity between the matrix and dispersed phases. The feasibility of the proposed technique was investigated through both a numerical simulation of the temperature field and an experimental study. The results of the simulation showed that the temperature increase of dispersed phase droplets with a diameter of approximately 200 μm was greater than 35°C in 0.1 s. An observational study of the test section also showed that the dispersed phase was considerably deformed by the selective heating. A precise measurement of the deformation and the diameters of the dispersed droplets showed that the radiation heating enhanced the distribution of the dispersed phase successfully. To investigate the droplet sizes, the experimental results were evaluated by plotting the capillary number with respect to the viscosity ratio of the blend. The results signified that the size of the dispersed phase was controlled successfully, which was estimated by the evaluation method used for a conventional process. Finally, the proposed technique is highly beneficial, because it can achieve blend control independent of the mixing conditions. Moreover, the effect of weight percentage of the dispersed phase on the selective heating will be investigated in future to extend this method to the actual processing.

REFERENCES

1. Utracki, L. A.; Polymer Alloys and Blends: Thermodynamics and Rhelogy; Hanser Publisher: Munich/New York, **1989**, p 13.
2. Sivaraman, P.; Chandrasekhar, L.; Mishra, V. S.; Chakraborty, B. C.; Varghese, T. O. *Polym. Test.* **2006**, *25*, 562.
3. Mouzakis, D. E.; Papke, N.; Wu, J. S.; Karger-Kocsis, J. *J. Appl. Polym. Sci.* **2001**, *79*, 842.
4. Bucknall, C. B. In Polymer Blends and Mixture; Walsh, D. J., Higgins, J. S., Maconnachie, A., Eds.; Martinus Nijhoff Publishers, **1985**; NATO ASI Series, Series E: Applied Sciences, No. 89, p 349.
5. Utracki, L. A. *Poly. Eng. Sci.* **1995**, *35*, 2.
6. Jarus, D.; Summers, J. W.; Hiltner, A.; Baer, E. *Polymer* **2000**, *41*, 3057.
7. Hong, J. S.; Namkung, H.; Ahn, K. H.; Lee, S. J.; Kim, C. *Polymer* **2006**, *47*, 3967.
8. Elias, L.; Fenouillot, F.; Majeste, J. C.; Cassagnau, Ph. *Polymer* **2007**, *48*, 6029.
9. Filipe, S.; Maia, J. M.; Leal, C. R.; Cidade, M. T. *J. Appl. Polym. Sci.* **2007**, *105*, 1521.
10. Sun, X.; Isayev, A. I. *Rubber Chem. Technol.* **2008**, *81*, 19.
11. Isayev, A. I.; Kumar, R.; Lewis, T. M. *Polymer* **2009**, *50*, 250.
12. Sundararaj, U.; Macosko, C. W. *Macromolecules* **1995**, *28*, 2647.
13. Grace, H. P. *Chem. Eng. Commun.* **1982**, *14*, 225.
14. Wu, S. *Polym. Eng. Sci.* **1987**, *27*, 335.